Nonlinear Optics and Quantum Optics, Vol. 41, pp. 27–57
Reprints available directly from the publisher
Photocopying permitted by license only

Photoinduced Deformations in Azobenzene Polymer Films

M. SAPHIANNIKOVA[1], V. TOSHCHEVIKOV[1,2] AND J. ILNYTSKYI[3]

[1]*Leibniz Institute of Polymer Research, 01069 Dresden, Germany*
E-mail: grenzer@ipfdd.de
[2]*Institute of Macromolecular Compounds, 199004 Saint-Petersburg, Russia*
[3]*Institute for Condensed Matter Physics, Lviv, Ukraine*

Received: July 27, 2009. Accepted: November 8, 2009.

This review is devoted to the microscopic mechanism behind photoinduced deformations in side-chain azobenzene polymers. We present the analysis of selected experiments that allows us to propose main criteria for a proper choice of the light induced force. Particularly, we provide convincing evidence that, contrary to a well-spread belief, light induced softening is a very weak accompanying effect rather than a necessary condition for the formation of surface relief gratings. Hence, the theories which need a concept of photo-induced softening are not able to describe the phenomenon correctly. Using molecular dynamics simulations, we show that chromophore reorientation alone is capable of the film deformation under homogeneous illumination. Finally, we discuss a recent microscopic theory that satisfies all main criteria for a proper choice of the light induced force. The theory is based on the orientation mechanism of azobenzene chromophores and takes the internal structure of side-chain azobenzene polymers explicitly into account.

Keywords: Azobenzene polymers, surface relief gratings, light-induced stress, molecular dynamics simulations, microscopic theory.

1 INTRODUCTION

The role played by azobenzene polymers in the modern photonic, electronic and opto-mechanical applications cannot be underestimated. These polymers are successfully used to produce alignment layers for liquid crystalline fluorescent polymers in the display and semiconductor technology [1, 2], to build waveguides and waveguide couplers [3, 4], as data storage media [5–8] and as labels in quality product protection [9]. A very hot topic in modern research

are light-driven artificial muscles based on azobenzene elastomers [10–12]. Some attempts are made to use azobenzene polymers as structured templates for production of 3D photonic crystals [13, 14].

The incorporation of azobenzene chromophores into polymer systems via covalent bonding [15, 16] or even by blending [17–19] gives rise to a number of unusual effects under visible and ultraviolet irradiation. While light-induced reorientation of azobenzene chromophores in the polymer matrix is now considered to be a well-understood process, the light-induced changes of the matrix itself have been a puzzling phenomenon since the discovery in 1995 [20, 21]. A satisfying explanation represents a great challenge for the azobenzene community and upon solving will definitely become a milestone in development of the modern polymer physics.

The most astonishing effect is the inscription of surface relief gratings (SRGs) onto thin azobenzene polymer films [20–23]. It is usually performed by exposing the sample to periodic intensity or polarization pattern resulting from the interference of two polarized laser beams. The absorption of light at a wavelength of about 480 nm induces material flow even at room temperature, several tens of Kelvin below the glass transition temperature, T_G, of the polymers. Another interesting and relative effect is photo-induced deformation of azobenzene polymer films floating on a water surface. It has been shown by Bublitz *et al*. [24] that different types of azobenzene side-chain polyesters undergo an opposite change of shape under illumination with linear polarized light. This result is in agreement with the observation that the phase of the SRGs, relative to that of the optical grating, strongly depends on the chemical architecture of the particular azobenzene polymer [3, 25]. In this review we shall show that, if one would understand the microscopic mechanism behind the uniaxial deformation of free-standing films in the key experiment of Bublitz *et al.* [24], one will also understand the origin of light induced force behind inscription of SRGs.

We shall start our review (Section 1) from brief description of structure and properties of azobenzene polymers and influence of their molecular weight and degree of functionalization on the SRG formation. At the end of Section 1 we shall explain the orientation mechanism of azobenzene chromophores under illumination with the polarized light.

Section 2 will be devoted to the analysis of select experiments that allows us to propose three main criteria for a proper choice of the light induced force. First, we shall provide convincing evidence that, contrary to a well-spread belief, light induced softening is a very weak accompanying effect rather than a necessary condition for the formation of SRGs. This key finding implies that a light induced stress should lie above the yield point of the azobenzene polymer in order to cause the macroscopic transport well below the glass transition temperature. Additionally, we shall show that the light induced stress strongly depends on the chemical architecture of azobenzene molecules as well as on the temperature at which the inscription of SRG is done.

Section 3 will be devoted to molecular dynamics simulations of side-chain azobenzene polymers. These simulations allowed us to verify the microscopic mechanism behind the light induced stress. The simulations were carried out on two model side-chain azobenzene polymers [26–28]. The first one has a stiff main chain and a short spacer, while the second one has a flexible main chain and a long spacer. In both cases the only effect of the illumination that was taken into account was the reorientation of the trans-isomers of azobenzene perpendicularly to the polarization of the light. Both models demonstrate a noticeable deformation under homogeneous illumination, but the sign of deformation is different depending on the molecular architecture. Hence, our computer simulations provide a crucial proof that the force leading to uniaxial deformation of free-standing films may originate solely from the light-induced orientation of azobenzenes.

In Section 4 we shall discuss a recent microscopic theory that satisfies all three criteria for a proper choice of the light induced force. The theory is based on the orientation mechanism of azobenzene chromophores and takes the internal structure of side-chain azobenzene polymers explicitly into account. It is shown that reorientation of azobenzenes results in the orientation anisotropy of main chains which is accompanied by the appearance of mechanical stress. The microscopic theory is the first theory which provides the value of the light-induced stress larger than the yield stress. Thus, this result explains a possibility for the inscription of surface relief gratings in glassy side-chain azobenzene polymers.

At the end of this review we shall briefly summarize our present understanding of this complicated and rather controversial topic and also provide some perspectives of its future development.

1.1 Structure and properties of azobenzene polymers

The class of azobenzene polymers is represented nowadays by a wide variety of chemical structures (for review see Refs. [3] and [29]): starting from guest-host systems in which an azobenzene dye is doped into the polymer matrix and thus is prone to agglomeration at higher concentrations [30–32], through functionalized homo- and co-polymers with side-chain azobenzene chromophores, and finally reaching a complexity of such supramolecular structures as azobenzene polymer networks which can be considered as a cross-linked modification of the two first types. While the scientific interest to uncrosslinked azobenzene polymers is gradually waning, the networks systems has been recently receiving a great and constantly growing attention as very promising templates for production of artificial muscles (attenuators) [10, 11, 33]. The main-chain azobenzene polymers have been also synthesized in the beginning of azobenzene era but it was very soon realized that these systems do not exhibit pronounced orientational and deformational effects, as the mobility of azobenzenes is considerably restricted by their inclusion into the polymer backbone [3]. An attempt was also made to use branched and even dendritic

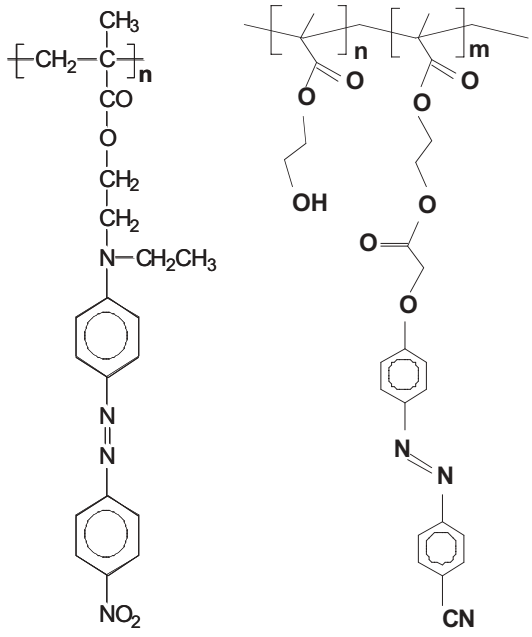

(a) (b)

FIGURE 1.1
The chemical structure of amorphous azobenzene polymers used in this study: (a) homopolymer pDR1M, $T_G = 130\,^{\circ}C$; (b) statistical copolymer pCM1, $T_G = 90\,^{\circ}C$.

polymer structures [34, 35] but again the effects observed were considerably smaller than those in linear azobenzene polymers.

Depending on the length of the spacer, the side-chain azobenzene polymers can be roughly subdivided into amorphous polymers with a short spacer (2–3 methylene groups) and liquid crystalline polymers [34, 36] with a long spacer (6–10 methylene groups). The original experimental results discussed in this study were obtained with two types of amorphous polymers (Fig. 1.1). One is a well-known homopolymer pDR1M [poly((4-nitrophenyl) [4-[[2-(methacryloyloxy)-ethyl] ethylamino] phenyl] diazene)] originally synthesized in the group of Prof. Almeria Natansohn (Kingston College, Canada) and later reproduced in the group of Dr. Burkhard Schulz (Institute of Thin Film Technology and Microsensorics e.V. Teltow). Another is a statistical copolymer pCM1 [poly(2-hydroxyethyl)methacrylate-co-(2-(4-(4-cyanophenylazo)phenoxy) acetyl)methacrylate)] synthesized in the group of Prof. Henning Menzel (University of Braunschweig) [35]. Although optical properties of these systems as well as transient dipole moments of the isomers are quite different [37], both polymers have been successfully used for inscription of the SRGs with a similar efficiency at the conventional

illumination conditions (10 minutes, 100 mW/cm^2, 488 nm). The amine-substituted azobenzene derivative in pDR1M appears to be rather unstable under prolonged irradiation (30 minutes) at this wavelength due to oxidative degradation [38, 39]. It may thereby form other chemical products which presumably secure density changes that were found solely in PDR1M upon heating the polymer above the glass transition temperature [40, 41].

There is controversial information about the influence of the molecular weight on the efficiency of the SRG formation in the literature. First, the Natansohn's group reported on significant reduction of the inscription rate with the increasing molecular weight and even on total inhibition of the grating growth at molecular weights of 25 kg/mol and higher [42]. However, this result was obtained with the 1:1 blended films of PDR1A (PDR1M with the backbone methyl group substituted on hydrogen) and PMMA, the molecular weight of which was varied [22]. Thus, these data simply show that increasing number of entanglements in the host PMMA suppresses the grating growth. Later, the group of Tripathy managed to inscribe the SRGs in amorphous azobenzene polymers having very high molecular weight of more than 500 kg/mol, although the inscription was less efficient than for low molecular weight polymers [3]. Also, the systematic variation of the molecular weight of pCM1 (Fig. 1.1b, n=35% and m=65%) up to 200 kg/mol only slowed down the grating inscription, but did not inhibit it completely [43]. Concerning the influence of azobenzene content on the grating formation, here different groups agree that the inscription rate increases with the degree of functionalization in the statistical copolymers up to a certain threshold value that is above 40% and depends on the particular polymer [35, 44, 45]. After this threshold, the inscription rate is found to be either independent of the degree of functionalization [44] or shows a tendency to a small decrease [35, 45].

Presently, there is no doubt that multiple trans-cis and cis-trans photoisomerizations of the azobenzene moieties are the trigger of the inscription process. Though, it is not clear at all, what kind of microscopic mechanism is responsible for the inscription. Over the years, some of the proposed mechanisms, for example pressure gradients due to volume changes [22] or thermal gradients [46], had been rejected as they cannot explain some of the essential features of the SRG formation. Also, we showed that the electric force gradients, for some years the most favored model amongst experimentalists [47–50], are too small to be seriously taken into account [51]. What stays? Is it simply the mechanical switching between two isomerization states, the impulse of which, due to unknown reasons, pushes the chains to reptate in a particular direction defined by the light polarization (the model of anisotropic diffusion proposed by Lefin *et al.* [52, 53] in 1998 and revived by an unawared group of French scientists [54] in 2006 as the random-walk model of molecular motors). Or maybe, it is the orientation of chromophores that leads to the change in the intermolecular interactions of azobenzenes? In any case, only consideration of the photoisomerization process and its consequences,

shall deliver a first insight into the puzzle of the grating inscription in the azobenzene polymers.

Many optoelectronic applications of dye-containing polymers need some aligning of anisotropic or polar active molecules. The reversible trans-cis isomerization (E-Z isomerization) of azobenzenes induced by resonant excitation with a polarized laser beam is by far the mostly used mechanism due to its efficiency and of the good stability of azo-dyes. The polarized light imposes on anisotropic dye molecules an angular selective optical pumping that results in a macroscopic alignment perpendicularly to the light polarization [55, 56]. Only in the case of such orientation further absorption of photons is prevented and, hence, a steady state is reached [57, 58].

M. Dumont and E. Osman have introduced a theoretical "hole-burning" model for the simulation of photoinduced reorientation of azo-dyes in amorphous polymers [59, 60]. The mechanism of angular hole-burning model can be understood intuitively if one considers the probability of absorption. It is given by

$$P_J(\theta) = I_P \sigma_J [1 + \varepsilon a_J P_2(\cos\theta)] \tag{1.1}$$

where I_p is the pumping intensity in W/cm^2, $P_2(x) = (3x^2 - 1)/2$ is the second Legendre polynomial, σ_J and a_J are the average absorption cross section and the molecular anisotropy of trans (J=T) and cis (J=C) isomers, respectively. $\varepsilon = 2$ for linear polarized light, and $\varepsilon = -1$ for circular polarized light [60]. Let us consider the irradiation with linear polarized light and assume for simplicity that $a_T = a_C = 1$:

$$P_J(\theta) = 3 I_P \sigma_J \cos^2\theta \tag{1.2}$$

Hence, the probability of excitation by the linear polarized light is proportional to $\cos^2\theta$. Therefore, starting from a sample with an isotropic angular distribution of the chromophores, multiple trans-cis-trans photoizomerization with linearly polarized light will result in a preferential orientation of the long axis of the chromophores. After some time, a dynamic steady state will be established which is characterized by a rather small fraction of chromophores pointing in the polarization direction and thus a small photoizomerization rate (Fig. 1.2).

2 LIGHT INDUCED FORCE

Starting from 1998, several models [42, 47–50, 52, 53, 61–64] have been proposed to explain the origin of the inscribing force in azobenzene polymer films. However, none of them describes satisfactorily the light induced motion of the azobenzene polymers at a molecular level. If it would be the case, there will be no need in new theories which appear every second year. With growing

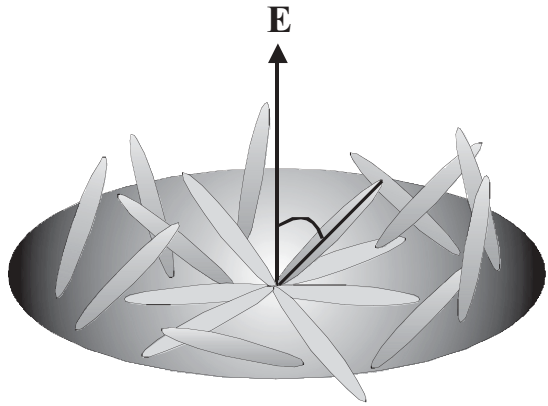

FIGURE 1.2
Azobenzenes with the long axis laying perpendicular to the electric field vector **E** represented here as gray rods cannot be excited.

number of model approaches, it becomes difficult to decide what kind of model is the most appropriate for description of light induced deformations.

This section intends to provide three main criteria for a proper choice of the light induced force. We base our analysis on a number of select experiments. The first experiments, carried out in the group of Dieter Neher at Potsdam University, show that effects of light induced softening as well as light induced diffusion can be neglected in azobenzene polymer films [65–69]. The second experiments, performed by Bublitz *et al.* [70], demonstrate a big influence of the molecular architecture on photoinduced deformations (rigidity of the main chain and the length of the spacer in side-chains). The third experiments, performed in the group of Ullrich Pietch at Siegen University, reveal a destructive effect of elevated temperatures on the inscription of surface relief gratings [71, 72].

2.1 Light induced softening and diffusion

In most models, to explain the mass transport over micrometer distances during irradiation at room temperature, it is necessary to assume a considerable degree of photoinduced softening, at least comparable with that at the glass transition. In other models [47, 49, 62], only the mechanism of SRG inscription is proposed without giving a force estimate. In this subsection we shall provide convincing evidence that there is no considerable softening of the azobenzene layers under illumination. This evidence was obtained using three different techniques operating at totally different time scales: electromechanical spectroscopy ($\sim 10^{-3}$ s), atomic force microscopy (~ 1 s) and fluorescence recovery after photobleaching ($\sim 10^{3}$ s).

It is well known that the Young's storage modulus increases exponentially with the frequency in dynamic mechanical measurements [73]. The sample

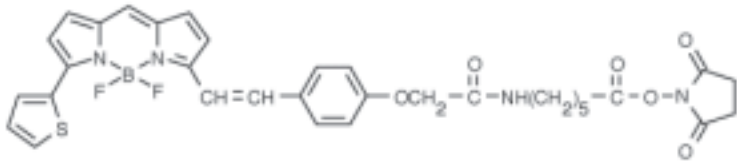

FIGURE 2.1
Chemical structure of the red-fluorescent dye D10000.

goes through the glass transition in much the same way as when the temperature is lowered. The quartz crystal resonance experiments from Srikhirin *et al.* [65] were carried out at very high frequencies of several GHz when predicted softening of the azobenzene polymer film under illumination with visible light would probably stay unnoticed. Electromechanical experiments from Mechau *et al.* were done at a much lower frequency of 2.5 kHz [66, 67]. Still only negligible changes in the plate compliance and in the dielectric constant were observed (10% under illumination against 1000% upon heating till T_G). With the force-distance mode of atomic force microscopy (AFM), in which a stress is applied quasi-statically at about 1 Hz, only a 50% decrease in the Young's modulus has been found under illumination with visible light [68].

The force-distance mode of atomic force microscopy operates at a frequency of about 1 Hz. As the polymer response strongly depends on the excitation frequency, it is worth to utilize another method performing at much lower frequencies. Therefore, Mechau *et al.* [69] have chosen a fluorescence recovery after photobleaching (FRAP) that operates at the range of minutes. The FRAP technique has been successfully used to measure the translational motion of tracer molecules in thin polymer films around the glass transition temperature [74–76]. The principle idea of this method is that small dye molecules are mixed to the polymer layer and then destroyed in some area by a burst of light. The photobleached area can then be scanned using a narrow beam of an appropriate wavelength that excites the undestroyed dye molecules which start to emit light. If with time undestroyed molecules diffuse into the photobleached area, the process of diffusion will manifest itself as a gradual increase in the fluorescent intensity.

The FRAP method has been chosen to follow changes in the viscosity of azobenzene layers at different temperatures and under illumination [69]. According to the free volume theory, the diffusivity of small molecules depends exponentially on the free volume fraction as a result of an exponential increase in the viscosity [73]. Therefore, already a minor increase in the free volume ($<5\%$) [77], e.g. induced by an increase in temperature above the glass transition temperature, is expected to cause a significant increase in the diffusivity.

The material investigated is statistical copolymer pCM1 (Fig. 1.1b) [35]. This polymer has a molecular weight of 8.6 kg/mol, an azobenzene content

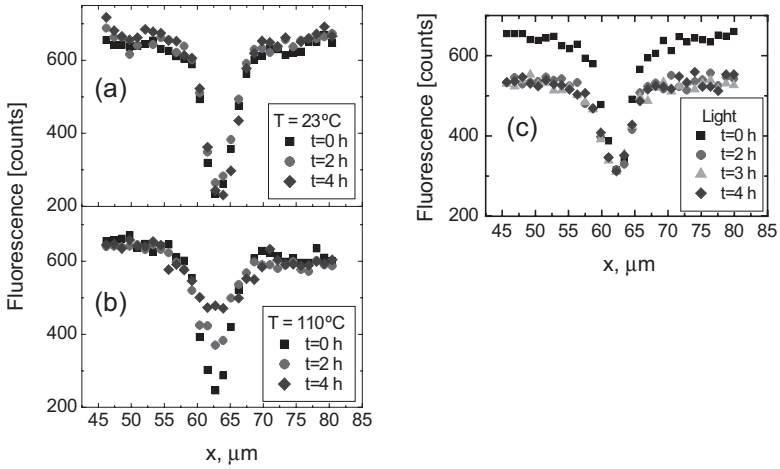

FIGURE 2.2
The profile and recovery of the bleached region at several times after the bleaching process of the azobenzene layer at room temperature (a), 20 °C above the glass transition temperature (b), under illumination with visible light at room temperature (c). Reprinted from Ref. [69] with permission from American Institute of Physics.

of 62% and $T_G = 90\,^{\circ}\mathrm{C}$. A commercial red-fluorescent dye, D10000 from "Molecular Probes", was used as the tracer molecules (Fig. 2.1). This dye exhibits an absorption maximum at 632 nm, well beyond the absorption of the azobenzene film. The emission of the dye in the polymer matrix is at 650 nm. To avoid aggregation of the dye molecules, only 0.01 wt% D10000 was mixed to the azobenzene polymer. Under these conditions, the fluorescence intensity of the dye was found to be only two times lower within azobenzene-containing layers compared to its value in an inert layer such as PMMA. Investigations of solutions containing both the dye and the azobenzene polymer showed a strong decrease in the fluorescence with increase of the azobenzene concentration. This indicates a certain degree of photoinduced charge transfer to the azobenzene as has been observed for other dye-doped azobenzene layers [78].

The translational diffusion of the dye molecules within the azobenzene layers was measured by the FRAP-technique. An initial "writing" step with high intensity light of a focused HeNe-laser ($\sim 10^8$ mW/cm^2) creates a spatial variation of the fluorescent dye concentration in the layer by local photobleaching. A second "reading" cycle creates a fluorescence intensity image by scanning the sample with an attenuated reading intensity of the same HeNe laser at a reduced intensity of $\sim 10^4$ mW/cm^2 across an area of ca. $40 \times 40\ \mu$m^2. The scanning and the fluorescence detection was done with a modified confocal Raman Spectrometer (Dilor).

Translation diffusion of the dyes can then be followed by measuring the fluorescence intensity profiles across the bleached region at successive times

at temperatures below and above T_G. At room temperature (23 °C), ca. 70 °C below T_G, the spatial fluorescence intensity of the bleached area did not change within hours (Fig. 2.2a). On the other hand, diffusion of dye molecules could be observed at a temperature of 110 °C, 20 °C above T_G (Fig. 2.2b). The diffusion coefficient, D, in the two-dimensional case can be calculated by using the Einstein relation: $D = a^2/(4\tau)$, where a^2 is the area of the bleached region, and τ is the time constant of the fluorescence recovery of the bleached region. The time constant was determined from the time dependence of the measured fluorescence recovery (Fig. 2.2b). With $\tau \approx 100$ min at 110 °C and a diameter of the bleached area of 4 μm the diffusion coefficient is calculated to be 7×10^{-11} cm^2/s. This compares well with values for the diffusion coefficient of small tracer molecules in a PMMA matrix above the glass transition temperature.

To test if tracer-diffusion can be caused by light well below T_G, similar experiments were performed while illuminating a large area of the layer, including the photo-bleached spot, with circular polarized light of an Ar^+ laser at a wavelength of 488 nm and a moderate intensity of 100 mW/cm^2. These parameters are usually used for the inscription of SRGs. Consequently, if an active light-induced change in the viscosity takes place at room temperature, it should be detectable by the initiation of the diffusion. However, the data in Fig. 2.2c clearly show that light-induced diffusion of the dye molecules within the polymer layer is absent under the above-mentioned conditions.

Interestingly, we found a distinct reduction of the fluorescence intensity if the homogenous illumination of the Ar^+ laser at 488 nm wavelength is switched on (Fig. 2.2c). We presume that this reduction is caused by an additional fluorescence quenching in the presence of cis-isomers of the azobenzene dye, which forms upon photo-isomerization. For a constant cis fraction during the illumination at 488 nm, the measured spatial fluorescence intensity remains constant (Fig. 2.2c). The absence of appreciable changes in the fluorescence intensity in the subsequent scanning cycles in Fig. 2.2c proves that the illumination with moderate intensities of 488 nm wavelength does not induce any dye diffusion within the azobenzene layers.

Additionally, we found that an illumination with linear polarized light does not lead to any demonstrable dye diffusion in any particular direction. The independence of the diffusion on the polarization conditions is in contradiction to the concept of photo-induced translational diffusion as proposed by Lefin *et al.* [52, 53] and of an anisotropic photo-fluidity as proposed later by Karageorgiev *et al.* [79] Based on the observation that the width of a scratch in an azobenzene layer was gradually reduced only when the light polarization was perpendicular to the scratch, the latter authors concluded that an azobenzene layer under illumination behaves like a fluid in the direction perpendicular to the light polarization and like a solid in the parallel direction. Contrary to this interpretation, our recent experimental and theoretical results provide a convincing evidence that it is dealt with a light induced

anisotropic stress rather than with light induced anisotropic material properties [37, 80, 81].

In conclusion, we showed in this subsection that photoisomerization of azobenzene at light intensities typically used for the SRG writing does not cause a softening of the polymer layers from the glassy to the melt state. Moreover, an illumination at several polarization conditions did not reveal any detectable change in the viscosity of azobenzene layers. This leads us to the conclusion that a light-induced stress should lie above the yield point of the azobenzene polymer to be able to cause the macroscopic transport.

2.2 Effects of the molecular architecture

Bublitz *et al.* [24] observed a very interesting effect studying the photoinduced deformation of azobenzene polymer films floating on a water surface. It has been demonstrated that different types of azobenzene side-chain polyesters undergo an opposite change of shape under illumination with linear polarized light. Amorphous polyester (with a stiff main chain and a short spacer in the side chains) elongates along the direction of the electric field vector, while liquid-crystalline polyester (with a flexible main chain and a long spacer) contracts in the same direction (Fig. 2.3) [24]. This result is in agreement with the observation that the phase of the SRGs, relative to that of the optical grating, strongly depends on the chemical architecture of the particular azobenzene

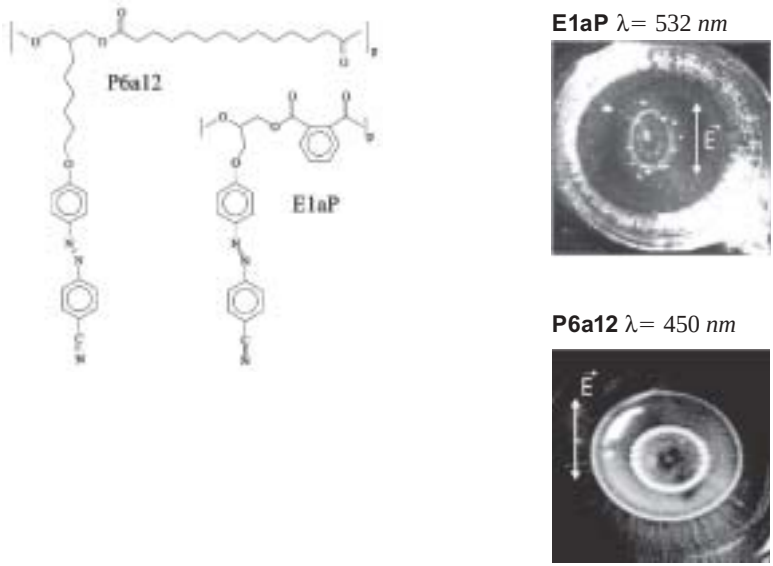

FIGURE 2.3
Chemical structures of liquid-crystalline P6a12 and amorphous E1aP polyesters (left) and the deformation of corresponding polymer films under illumination with linear polarized light (right). Reprinted from Ref. [24] with permission from Springer.

polymer [3]. Another related experiment was performed by Holme *et al.* [25], who illuminated the azobenzene film by a strip-like uniform light pattern formed due to the use of the optical mask [25]. Depending on the polymer architecture either peaks or trenches were observed in the illuminated strips. The authors also pointed out on the importance of the backbones rigidity, as for one particular architecture the peaks transformed into trenches when the aliphatic backbone was replaced by more rigid aromatic one [25].

Hence, both cases of spatially uniform and periodically modulated cases can be explained in terms of local deformations in polymer film under illumination, namely, the local compressions occur in LC systems and opposite effect of local extension takes place for amorphous azo-polymers. This means that the sign of light induced force is very sensitive to the molecular architecture.

2.3 Temperature effects

It is well known that surface relief gratings can be inscribed on polymer films containing azobenzene chromophores using a periodic holographic light pattern of wavelength around 500 nm [20–23]. This wavelength is close to the absorption maxima of the cis- and trans-conformations of azobenzene. Illumination of the polymer at this wavelength initiates the cis-trans and trans-cis photoisomerisation which results in a light-induced material transport far below glass transition temperature, T_G. Under continuous holographic exposure of thin polymer films Rochon *et al.* [20] and Kim *et al.* [21] observed the formation of surface relief gratings of nearly sinusoidal shape. Later it has been shown that the SRGs can be also inscribed using pulse like illumination, whereby the scattering signal exhibited first an instantaneous jump followed by a smaller slope of increase. If the actinic light is switched off the intensity decays exponentially to a level larger than that before the pulse. Depending on pulse duration and laser intensity the plastic deformation can be accumulated and the scattering intensity increases as function of the number of pulses [82].

In this subsection we describe the temperature resolved measurements performed recently by Veer *et al.* [71, 72]. These mesurements can help to clarify the process of elastic and plastic deformation caused by the light-induced ordering and thermally induced relaxation during grating formation. To study the temperature dependence of the grating formation, the pDR1M sample was heated steadily using a Peltier plate. To avoid the air turbulence, the experiment was performed inside a closed chamber at pressure of about 1000 Pa.

Figure 2.4 shows diffraction curves measured at different temperatures under continuous exposure with laser intensity $I_p = 1$ W/cm^2. It is clearly seen that the scattering intensity of the first order peak varies significantly with temperature. At $T = 25\,^{\circ}C$ one observes a typical inscription behavior: the intensity increases exponentially at the beginning and reaches saturation later. The intensity at saturation reflects the achieved formation of a nearly sinusoidal SRG. The measured intensity $I_1(t)$ is roughly proportional to the

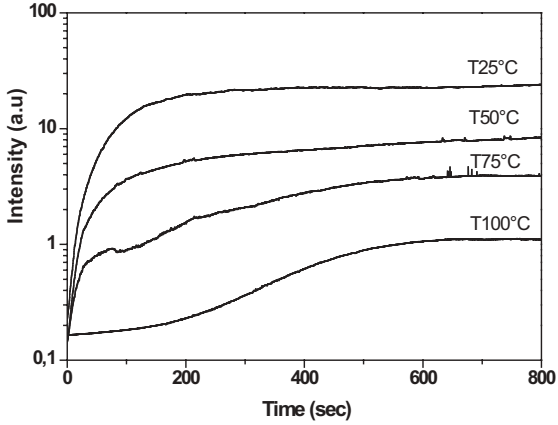

FIGURE 2.4
Temperature dependent intensity of the first order diffraction peak of the forming SRG grating measured using $\lambda_{probe} = 633$ nm. Reprinted from Ref. [71] with permission from Taylor & Francis.

square of the deformation and can be described by

$$I_1(t) = I_{sat}(1 - e^{-t/\tau_p}) \tag{2.1}$$

where I_{sat} is the intensity after saturation and $1/\tau_p$ is the rate of grating formation. The rate of grating formation $1/\tau_p$ can be extracted from the initial steepness of the diffraction efficiency curve. In contrast to room temperature, the efficiency of SRG formation is strongly reduced at higher temperatures. This is seen in the considerably reduced value of I_{sat} and in the lower slope of diffraction curves at the beginning of illumination. At $T = 100\,^{\circ}$C practically no gain is achieved.

Figure 2.5a shows the rate of grating formation, taken from the initial slope of the diffraction curve between $0 < t < 25$ s, as a function of temperature. It is found to decrease exponentially with the increase of temperature. The time constant of this exponential decay varies with the intensity of the inscribing laser (not shown). At about 100 °C the slope is almost flat. The AFM inspection shows that the grating height decreases linear with increasing temperature (Fig. 2.5b).

The development of SRG under pulse like exposure was investigated using a cyclic inscribing force by monitoring the 1st order diffraction intensity normalized to the intensity of the incident light, I_0. As in case of continuous exposure, the diffraction intensity varies with the temperature. This variation becomes very significant at higher temperatures. Here we show the results taken at $T = 80\,^{\circ}C$ up to T_G for the laser intensity $I_p = 1$ W/cm^2 (Fig. 2.6). Between the exposures the temperature was increased in steps of 5 °C. When the light is switched on, the diffraction intensity jumps to a certain value, then

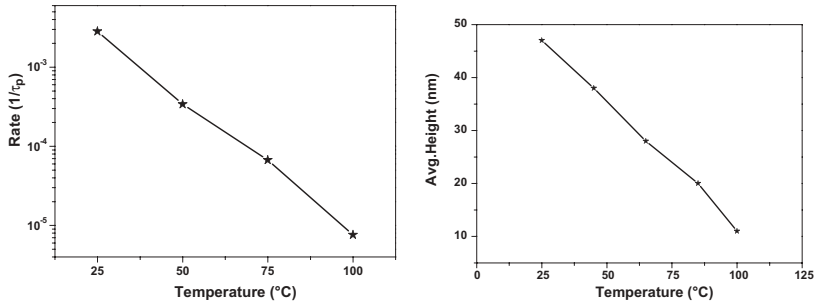

(a) (b)

FIGURE 2.5
Temperature dependent rate of the grating formation measured under continuous exposure (a). Temperature dependent grating height after continuous exposure, as measured using atomic force microscope (b). Reprinted from Ref. [71] with permission from Taylor & Francis.

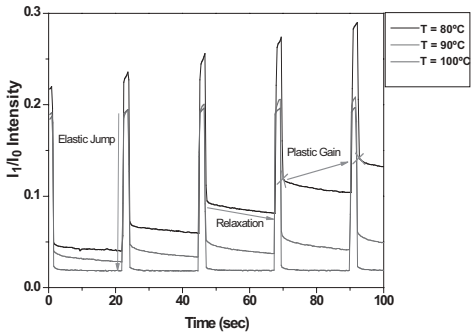

FIGURE 2.6
Pulsed exposure intensity of the first order diffraction peak, measured using $\lambda_{probe} = 633$ nm. Intensity of the inscribing laser is 1 W/cm^2. Reprinted from Ref. [71] with permission from Taylor & Francis.

increases further under illumination, and decays when the light is switched off. The difference in intensity between two subsequent pulses reflects the plastic gain in SRG formation. Subsequent pulses become accumulated which results in a stepwise increase of the grating height. The relaxation in dark shows exponential behavior as long as the temperature stays below 100 °C. At this temperature no plastic gain is found and also no relaxation is found. SRG grating is pure elastic and appears under green light only.

3 MOLECULAR DYNAMICS SIMULATIONS

This section is devoted to molecular dynamics simulations of side-chain azobenzene polymers performed by us in recent five years [26–28]. The main

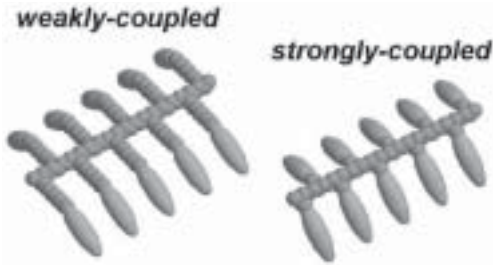

FIGURE 3.1
Weakly-coupled model (left), which represents the liquid-crystalline azobenzene polymer P6a12, and strongly-coupled model (right), which represents amorphous azobenzene polymer E1aP.

aim is to reproduce the key experiment of Bublitz *et al.* [24] (see Subsection 2.2) assuming that the chromophore reorientation is the primary source for the film deformation under homogeneous illumination. To describe principal differences between the chemical structures of the liquid-crystalline P6a12 and amorphous E1aP azobenzene polymers (Fig. 2.3 left), we consider two characteristic topologies. Both are of the side-chain type but different in both backbones rigidity and in a degree of elastic coupling between the backbone and the chromophore (Fig. 3.1), hence their names. A weakly-coupled model has a flexible, alkyl-like backbone and relatively long flexible spacer of 10 pseudo-atoms [26]. The strongly-coupled model, on contrary, has a very short spacer of two sites and both backbone and the spacers are made relatively rigid by increasing the barriers of torsional interactions. That was done in a view of the role that is played by the backbone rigidity, as being observed experimentally [25] and was already pointed out by us above. Both topologies has the same backbone length of 39 pseudo-atoms and the same number of ten side chains attached in a syndiotactic way.

The azobenzene moieties are represented in the MD simulations by the Gay-Berne rods [83]. In this study we used the following parametrization for the Gay-Berne potential, $\mu = 1$, $\nu = 2$, length-to-breadth ratio $\kappa = 3$, side-to-side/end-to-end well depth ratio $\kappa' = 5$, the length and energy scale parameters are $\sigma_0 = 5\,\text{Å}$ and $\varepsilon_0 = 0.561 \times 10^{-20} J$. The MD simulations are performed in $NP_{xx}P_{yy}P_{zz}T$ ensemble, where each component of the pressure $P_{\alpha\alpha}$ is controlled via separate Hoover barostat (for more details, see Ref. [27]). This allows anisotropic changes of the box dimensions to be monitored.

The photoisomerization of azobenzene is a complex quantum mechanical phenomenon which involves excitation of the electrons of the $N = N$ double bond and is on the time-scale of tens of picoseconds. However, from the perspective of our level of modeling, it can be considered as certain classical mechanics perturbation that acts on azobenzenes and initiate further mechanical changes in polymer structure. We assume that the material contains azobenzene with such chemical substituents that continuous cyclic trans-cis

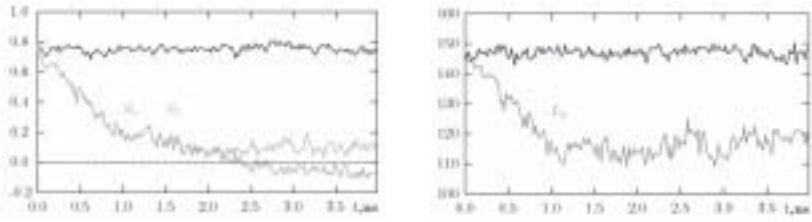

FIGURE 3.2
Order parameters (left) and box dimension along the field (right) evolution after applying weak effective field, $f = 0.2$. S_z is the order parameter along the field and S_2 is the usual nematic order parameter. Reprinted from Ref. [28] with permission from Taylor & Francis.

isomerization occurs under illumination and the photostationary state with preferential orientation of azobenzenes perpendicular to the light polarization can be established (see Section 1). This effect can be modeled by applying the effective light induced field directed along the light polarization and introduced via an extra energy term $U = U_0 P_2(\cos\Theta)$. Further, the reduced field strength, f, where $U_0 = f \times 10^{-20}\ J$ will be used.

3.1 Weakly coupled model

For the weakly-coupled model we analyzed the effect of external field on smectic A phase which is build at $T = 485\ K$ (just below T_{SI}) following the method described in Ref. [27]. The simulation box contained 64 molecules with total number of 8896 polymer beads and 640 mesogens, the box dimensions are of the order of 100 Å. The direction of field is chosen to be parallel to the mesogens director (this corresponds to the experimental situation of light beam hitting polymer film with planar arrangement of mesogens). Two different scenarios are observed in the weak field ($f = 0.2$) and the strong field ($f = 1.5$). In the weak field, the only effect observed is field-induced smectic-isotropic transition (Fig. 3.2 left). On the same time scale we observe contraction of the box along the field, due to repacking of the mesogens (Fig. 3.2 right). This effect is observed experimentally in nematic films under spatially modulated illumination when the film is examined by polarizing optical microscope [84]. It also reproduces anisotropic shrinking of the P6a12 freely floating drop along the light polarization [24]. One should mention that the same effect would be observed in polydomain film, but to smaller extent, as only fraction of chromophores will be repacked.

If the strength of the field increases, the second effect takes place, namely, the smectic phase is regrown with different spatial arrangement of the layers, where the mesogens now are perpendicular to the field (Fig. 3.3). One should mention that shrinking of the polymer along the film takes place mainly due to the smectic-isotropic (could be nematic-isotropic in other polymers) transition. In this respect, inclusion of the cis-isomer (these are not included in our study explicitly) will amplify this transition further.

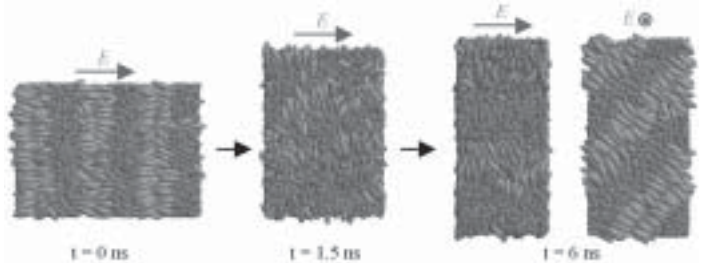

FIGURE 3.3
Snapshots that demonstrate field-induced sequence of phase changes in strong field, $f = 1.5$, first smectic-isotropic transition and then isotropic-smectic transition with rearranged layers. Reprinted from Ref. [28] with permission from Taylor & Francis.

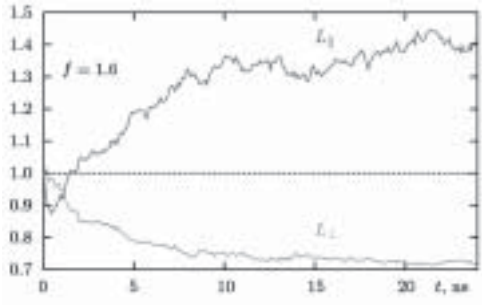

FIGURE 3.4
Scaled box dimension along the field, $L_{\parallel}$, and averaged box dimensions perpendicularly to it, $L_{\perp}$, strongly-coupled model, $f = 1.6$. Reprinted from Ref. [28] with permission from Taylor & Francis.

3.2 Strongly coupled model

The strongly-coupled model does not exhibit the smectic phase, which is in agreement with typical experimental phase diagrams of side-chain LC polymers with short spacer [85]. We studied the field-induced deformations of this model at $T = 485\ K$, where the polymer is found in a polydomain phase. By applying the external field in certain interval of strengths, e.g. $f = 1.6$, at first some rapid contraction along the field is observed (similarly to the case of weakly-coupled model), and then slower but substantial extension of the box takes place (Fig. 3.4). The effect is also observed on the snapshots of the melt (Fig. 3.5).

We found the following microscopic mechanism for this effect. The deformations of backbones is excluded as the metrics properties of these, monitored via semiaxes of their equivalent ellipsoids, are unchanged (not shown here). Reorientation of the backbones happens on the same time scale as that for the mesogens (3–5 ns), whereas the dimension of the box grows for at least another 5 ns. Hence, the accumulated stress due to repacking of polymeric matrix is

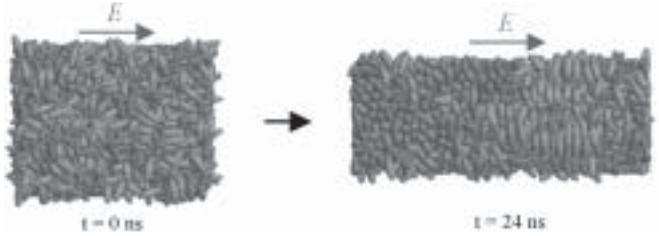

FIGURE 3.5
Snapshot for the field-induced extension of the sample, strongly-coupled model, f=1.6. Reprinted from Ref. [28] with permission from Taylor & Francis.

seen as the main driving force for the extension of the box. This is also confirmed by the fact that the box extends further for another 5ns after the field is switched off. As in the case of weakly coupled model, we should remark that the explicit existence of the cis-isomers in the model will not change the abovementioned mechanism. To conclude, by constructing strongly-coupled model we are able to reproduce the anisotropic deformation of free-floating amorphous polymers [24] by taking into account solely the reorientation of the trans-isomers of the chromophores.

Thus, we found out that both models demonstrate deformation under homogeneous illumination with the visible light, but the sign of deformation is different depending on the molecular architecture. It means that the experiments under uniform illumination, including those by Bublitz *et al.* [24] and Holme *et al.* [25], can be reproduced in the computer simulations without assuming dipole-dipole forces [63] or the anisotropic steps performed by molecular motors [52, 54]. Though, these non-polymer models may explain formation of the weak surface relief gratings in a number of glass-forming low molecular weight compounds with incorporated azobenzene groups [54, 86].

4 MICROSCOPIC THEORY OF LIGHT INDUCED DEFORMATION

Several models [42, 47–50, 52, 53, 61–64] have been proposed to explain the origin of the inscribing force. Most models [42, 47, 48, 50, 52, 63, 64] provide values of the light-induced stress ($\sigma < 1\ kPa$) much smaller than values of the yield stress typical for glassy polymers, $\sigma_Y \sim 10\ MPa$ [51, 68]. Therefore, to explain the origin of the inscription of SRGs many authors use a concept of photo-induced softening originally proposed by Tripathy and coworkers [47]. According to this concept, illumination of an azobenzene polymer layer with visible light induces a transition into a macroscopic low-viscosity melt and such a “molten” polymer can be then irreversibly stretched upon application of a very weak light-induced stress, $\sigma < 1\ kPa$. However, as we discussed in Section 2 three different experimental techniques unambiguously show

that illumination with a visible light does not affect material properties of an azobenzene polymer such as bulk compliance, Young modulus and viscosity [67–69, 87]. Therefore, one can certainly claim that the polymer remains in a glassy state and, hence, the theories which need a concept of photo-induced softening are not able to describe correctly the phenomenon.

On the other side, Saphiannikova and Neher [80] have recently proposed an alternative thermodynamic approach which explains the formation of surface relief gratings in the absence of photo-induced softening. This approach is based on the striction effect, namely, that orientation anisotropy of molecules in solids is accompanied by the appearance of mechanical stress. A well-known example is the electrostriction effect for solid dielectrics [88], where deformation is caused by external electric field. Another important example is spontaneous stretching of liquid crystalline elastomers where the elongation is due to intermolecular orientation interactions [89–91]. In the case of azobenzene polymers, the orientation anisotropy of polymer chains is caused by the photo-induced reorientation of chromophores. In the thermodynamic approach of Saphiannikova and Neher [80], starting from an anisotropic orientation distribution of chromophores, the light-induced stress comparable with the yield stress typical for glassy polymers has been obtained at some strengths of the light-induced alignment. However, it has not been shown how the strength of light-induced alignment depends on intensity of the laser light used for the inscription of SRGs. Moreover, neither the recent thermodynamic theory [80] nor the previous theories [42, 47, 50, 52, 61–64] are able to explain the well-known fact that photo-elastic properties of azobenzene polymers are very sensitive to the chemical architecture of macromolecules.

In order to overcome these drawbacks, Toshchevikov *et al.* [81] proposed recently a microscopic approach for description of light-induced deformations in side-chain azobenzene polymers. It is the first time when the internal architecture of azobenzene macromolecules, i.e. orientation distribution of chromophores with respect to the main chain, is explicitly taken into account. The sign of the light-induced stress has been found to be very sensitive to the internal architecture of side-chain azobenzene macromolecules due to the elastic coupling of chromophores to the polymer backbones. In this section we describe briefly the main assumptions behind the microscopic theory of Toshchevikov *et al.* [81] and its essential findings.

4.1 Microscopic model

We start from referring to the experimental fact that interaction of chromophores with linearly polarized light leads to the perpendicular alignment of long axes of the chromophores with respect to the electric vector **E** of the linearly polarized light (see Section 1). The effective light induced orientation potential has the following form [26, 92]

$$V(\Theta) = V_0 \cos^2 \Theta. \tag{4.1}$$

where V_0 is the strength of potential and Θ is the angle between the long axis of the chromophore and the vector **E** (Fig. 1.2). The value of V_0 is determined by the intensity of the laser light I_p and can be estimated as [71, 92]:

$$V_0 = \frac{1}{2} a \upsilon \tau \; I_p \equiv C \cdot I_p, \tag{4.2}$$

where a is the absorption coefficient, υ is the volume of azobenzene and τ is the effective transition time between two isomer states. For characteristic laser intensities $I_p \sim 1 \; W/cm^2$ and for the room temperature one can find in literature, $V_0 \sim 10^{-19} J$ [26, 71, 92], so that the coefficient of proportionality $C \sim 10^{-19} J \cdot cm^2/W$.

Interaction of chromophores with the polarized light results in the orientation anisotropy of polymer chains due to covalent bonding of chromophores to the chain backbones. We model here each azobenzene macromolecule as a rigid rod which bears a number of rod-like chromophores in side chains (Fig. 5.1). For short macromolecules, whose length is comparable with the Kuhn segment (such macromolecules were used, for example, in experiments [9, 51] and computer simulations [26]), the rods in our model describe orientation of stiff oligomers. For long azobenzene macromolecules [67, 69, 93], the rods imitate the orientations of freely-jointed Kuhn segments which form polymer chains. Thus, the formalism developed below can be applied for side-chain azobenzene polymers of different molecular weights.

Effective potential U of an oligomer in the field of the light wave is a sum of energies of chromophores inside the oligomer in the electric field. Orientation of an oligomer in space is defined by the angles θ, φ and ψ (Fig. 5.1a): θ is the angle between a long axis of an oligomer and the vector **E**, φ determines rotation of the oligomer around the vector **E**, ψ defines rotation of the oligomer around its long axis. We note that due to axial symmetry of the system, the potential U is independent of the angle φ and, using Equation (4.1), it can be written as

$$U(\theta, \psi) = N_{\text{ch}} V_0 \left\langle \cos^2 \Theta(\theta, \psi) \right\rangle. \tag{4.3}$$

Here N_{ch} is the number of chromophores in each oligomer and averaging runs over all chromophores inside the oligomer, whose orientation is defined by the angles θ and ψ. The average value of $\cos^2 \Theta(\theta, \psi)$ is determined by the orientation distribution $W(\alpha, \beta)$ of chromophores inside the oligomer. Here the angles α and β define the orientation of a chromophore in the frame of reference related to the oligomer: α is the angle between the long axes of a given chromophore and of the oligomer; the angle β is measured from a fixed axis Oξ perpendicular to the main chain of the oligomer (Fig. 5.1b).

4.2 Free energy and striction stress

In this subsection we outline the basic idea for calculating the mechanical stress appearing in a polymer sample under illumination with linear polarized light.

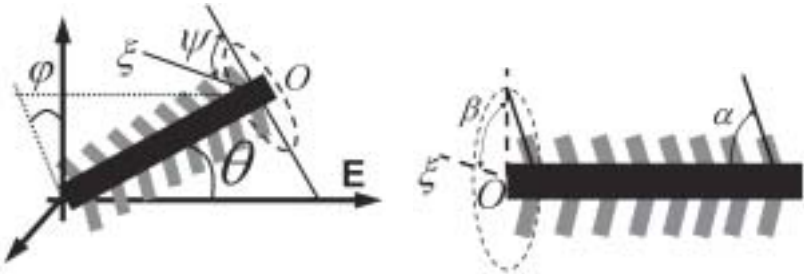

(a) (b)

FIGURE 5.1
Orientation of oligomer in space is defined by the set of three Euler angles $\Omega \equiv (\theta, \varphi, \psi)$ (a). Chemical architecture of oligomer is defined by the orientation distribution $W(\alpha, \beta)$ of chromophores inside the oligomer, i.e. by the potentials of internal rotations of the spacers (b). Reprinted with permission from Ref. [81]. Copyright 2009 American Chemical Society.

The idea is based on the well-known fact [88–90] that orientation anisotropy of molecules in a system leads to the appearance of the mechanical stress. The value of the stress, σ, is determined by the free energy of the system, F, which is found as a function of the strain, ε, [94]:

$$\sigma(\varepsilon) = -\frac{\partial F(\varepsilon)}{\partial \varepsilon}. \tag{4.4}$$

It should be noted that due to homogeneity of the light irradiation, no internal stress gradient exists which could lead to the translation movement of molecules in a homogeneous sample. Thus, one can certainly claim that the stress appearing in a homogeneous sample affected by a homogeneous laser beam is of "orientation" origin only. In such approach, the free energy is determined only by the orientation distribution of the oligomers, $f(\theta, \psi)$, and does not include contributions from translational movement of molecules. Hence, we can write the free energy as

$$F = nkT \int d\Omega f(\Omega) \ln f(\Omega) + n \int d\Omega f(\Omega) U(\Omega) + \frac{E\varepsilon^2}{2}, \tag{4.5}$$

where n is the number of oligomers in a unite volume. Here we set $\Omega \equiv (\theta, \psi)$. Integration in Equation (4.5) runs over the angles θ and ψ: $d\Omega = \sin\theta d\theta d\psi, \theta \in [0, \pi], \psi \in [0, 2\pi]$. The first term in Equation (4.5) is the orientation entropy of oligomers. The second and third terms are the energy contributions. The second term is the energy of all chromophores in the field of the light wave. The third term is caused by the elasticity of a glassy polymer, with E being the elastic Young modulus. We note here that the relative elongation, ε, of an azobenzene polymer is also of the "orientation" origin. Elongation of the sample is accompanied by the reorientation of oligomers and it is this reorientation which demands energy costs $E\varepsilon^2/2$ due to intermolecular

interactions between oligomers, whose rotational mobility is prevented in a glassy state. Therefore, ε is uniquely determined by the orientation distribution function of the oligomers, $f(\theta, \psi)$, and we can write ε as follows [81]:

$$\varepsilon = \varepsilon_{\max} \int d\Omega f(\Omega) P_2(\theta) \quad \text{with } P_2(\theta) = (3\cos^2\theta - 1)/2. \tag{4.6}$$

Here $\varepsilon_{\max}$ is the maximal strain corresponding to the fully oriented sample. It can be shown that the sign of the equilibrium elongation under illumination of the laser light coincides with the sign of the so-called striction stress, σ_{str}, at $\varepsilon = 0$. Hence, estimation of the value of the striction stress as a function of the field strength, $\sigma_{\text{str}} = \sigma_{\text{str}}(V_0)$, has been one of the important tasks of the microcopic theory [81].

4.3 Main results of microscopic theory

We do not want to go here into more details and refer an interested reader to the original work [81]. Here we briefly discuss the main results.

It has been found that the dependence of striction stress σ_{str} on the field strength V_0 has two different regimes:

$$\sigma_{\text{str}}(V_0) \cong \begin{cases} n_0 V_0 \dfrac{3\langle \sin^2\alpha\rangle_W - 2}{3\varepsilon_{\max}}, & N_{\text{ch}} V_0/kT < 1 \\ n_0 V_0 \dfrac{3\langle \sin^2\alpha\rangle_W - 2 - \left|\left\langle \sin^2\alpha \cos 2\beta \right\rangle_W\right|}{3\varepsilon_{\max}}, & N_{\text{ch}} V_0/kT \gg 1 \end{cases} \tag{4.7}$$

At small values of V_0 the sign of the striction stress, and thus the sign of sample elongation (stretching, $\varepsilon > 0$, or uniaxial compression, $\varepsilon < 0$) coincides, according to Equation (4.7), with the sign of a simple factor:

$$\text{C1} = \text{sign}\left[\langle \sin^2\alpha\rangle_W - 2/3\right]. \tag{4.8}$$

This means that the photo-elastic behavior of azobenzene polymers at small laser intensity is determined by the average angle α between chromophores and the main chain and does not depend on the distribution of chromophores with respect to the azimuthal angle β. For instance, if chromophores are attached to the backbone via short and rigid spacers so that the angle α is fixed, $\alpha = 90\,^\circ$ (Fig. 3.1 left), we have $\langle \sin^2\alpha\rangle_W = 1$, i.e. $C1 > 0$ and a sample is stretched along the vector **E**. This kind of behavior was found recently in computer simulations of azobenzene molecules with rigid spacers [28]. If the spacers are long enough (Fig. 3.1 left), chromophores can be positioned at some equiprobable angles α_* and $180\,^\circ - \alpha_*$ with respect to the main direction of the backbone. In this case $\langle\alpha\rangle = 90\,^\circ$, but $\langle \sin^2\alpha\rangle_W = \sin^2\alpha_* < 1$, so we have $C1 < 0$ and a sample is uniaxially compressed along the vector **E**. The striction stress obeys a linear dependence on the field strength at small laser

intensity. The condition $N_{\rm ch}V_0/kT < 1$ in Equation (4.7) corresponds to the light intensities $I_p < 5\ mW/cm^2$ at the room temperature and for $N_{\rm ch} \sim 20$, as it follows from Equation (4.2). These findings are in agreement with an experiment of Fukuda *et al.* [44] which demonstrates a linear dependence of sample elongation on the light intensity at $I_p < 5\ mW/cm^2$. However, at higher light intensities a non-monotonic dependence of sample elongation on the light intensity has been found experimentally [44, 48].

At high values of V_0 the sign of the striction stress coincides, according to Equation (4.7), with the sign of a factor:

$$C2 = \text{sign}\left[3\langle\sin^2\alpha\rangle_W - 2 - \left|\langle\sin^2\alpha\cos 2\beta\rangle_W\right|\right]. \tag{4.9}$$

This means that the photo-elastic behavior of azobenzene polymers at high laser intensity is strongly sensitive to the azimuthal distribution of chromophores inside the oligomers. If $C2 > 0$ the sample is stretched at high light intensities, $\sigma_{\rm str} > 0$. On the contrary, if $C2 < 0$ the sample is uniaxially compressed along the electric vector **E**, $\sigma_{\rm str} < 0$. This results in three types of the photo-elastic behavior of azobenzene polymers depending on their chemical architecture. If the condition $C1 < 0$ is fulfilled, a sample is monotonically compressed with increasing light intensity. If $C1 > 0$ and $C2 > 0$, the sample is monotonically stretched with increasing light intensity both at small and at large V_0. But if $C1 > 0$ and $C2 < 0$, sample elongation demonstrates non-monotonic dependence on V_0: at small V_0 a sample is stretched, whereas it is uniaxially compressed at large V_0. As example, we illustrate such non-trivial photo-elastic behavior for oligomers with fixed angles, $\beta = \pm\beta_*$, and $\alpha = \alpha_*$, $180^\circ - \alpha_*$. The dependences $\sigma_{\rm str}(V_0)$ for different values of α_* and β_* have been calculated numerically and are shown in Fig. 5.2. Figure 5.3 shows three areas on the plane $\alpha_* - \beta_*$ where the above mentioned conditions for α and β take place.

We note, that the non-monotonic photo-elastic behavior of azobenzene polymers has been observed in experiments. For instance, one can see in Figs 5 and 6 of ref. [44] a non-monotonic behavior of the inscription rate with increasing light intensity: the inscription rate increases at $I_p < 10\ mW/cm^2$, whereas it starts to decrease at $20\ mW/cm^2 < I_p < 100\ mW/cm^2$. Tripathy and coworkers [48] showed that the extension of a film can even change its sign at very high light intensities, $I_p \sim 100\ W/cm^2$. One can see from Figs 4 and 5 of ref. [48] that at $I_p < 1\ W/cm^2$ a film illuminated with a polarized Gaussian beam has a trench at the maximum of light intensity, i.e. a film is locally stretched along the light polarization **E**. However, at high light intensities, $I_p \sim 100\ W/cm^2$, a local peak is observed on a film surface, i.e. the film is locally compressed along the vector **E**.

We conclude this subsection section by noting that for all values of α_* and β_* the absolute value of the striction stress $\sigma_{\rm str}$ is described at large field strengths V_0 by the linear relationship $|\sigma_{\rm str}| \sim n_0 V_0$ according to

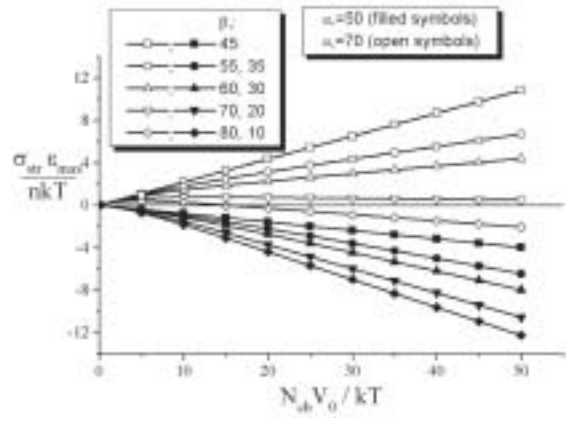

(a)

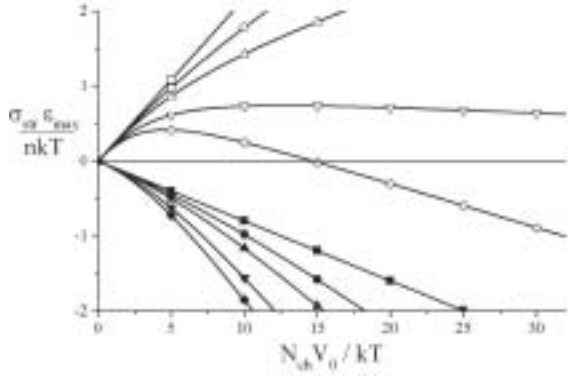

(b)

FIGURE 5.2
Dependences of the striction stress on the field strength $\sigma_{\rm str}(V_0)$ at different values of the structural angles α_* and β_*: the scale is small (a) and the scale is large (b). Reprinted with permission from Ref. [81]. Copyright 2009 American Chemical Society.

Equation (4.7). This relationship provides the values of the striction stress $\sigma_{\rm str} \sim 100\ MPa$ greater than the yield stress, $\sigma_Y \sim 10\ MPa$, at $I_p = 1\ W/cm^2$ and at the number density of azobenzenes $n_0 \cong 1.5 \times 10^{21} cm^{-3}$ typical for these materials. Thus, the microcopic theory [81] explains the possibility for irreversible inscription of surface relief onto azobenzene polymers of *any* chemical architecture. The same theory, using a visco-plastic approach, allows to show that the irreversible elongation of a sample decreases with the increasing temperature. The critical temperature, when the irreversible elongation disappears, is independent of the glass-transition temperature, T_g, and can be

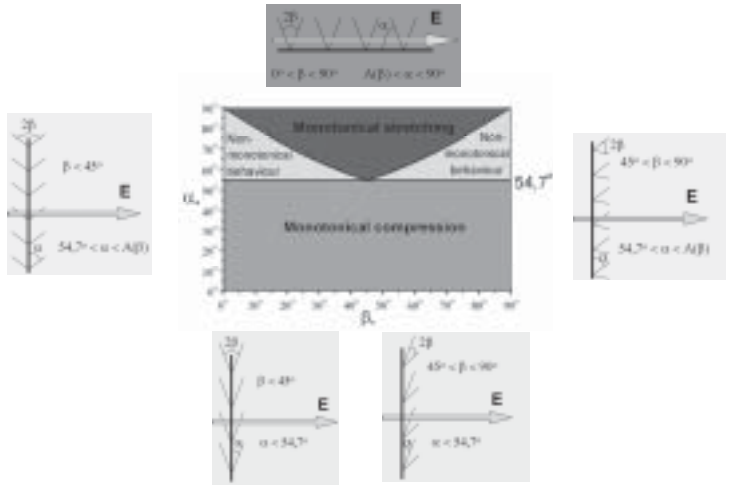

FIGURE 5.3
Three areas of the values of the structural angles α_* and β_* (Fig. 5.1b) for three typical deformation behaviors. Also, the corresponding architectures and orientations of oligomers with respect to the electric field **E** are shown.

smaller than T_g. This result is in accordance with the temperature-dependent measurements of Veer *et al.* [71, 72] discussed in Subsection 2.3.

5 SUMMARY AND OUTLOOK

Until recently, formation of the surface relief gratings has been mainly studied on the macroscopic level which inevitably lead to less or more severe assumptions in the existing theoretical models. It is however clear that further progress in understanding of this puzzling phenomenon cannot be achieved without studies on the microscopic level. Here, computer simulation methods offer a number of advantages in comparison with the conventional experimental methods [95, 96]. Realizing this, we launched in 2005 robust MD simulations utilizing the program that was developed for liquid crystalline polymers with arbitrary topology [97, 98]. The main aim was to reproduce the experiment of Bublitz *et al.* [24] (see Subsection 2.2) assuming that the chromophore reorientation is the primary source for the film deformation under homogeneous illumination. The simulations demonstrated a noticeable deformation of two model side-chain azobenzene polymers [26–28] with the sign of deformation being different for the weakly-coupled and strongly-coupled model. Hence, the experiment of Bublitz *et al.* [24] can be reproduced in the MD simulations using only the mechanism of azobenzene reorientation.

The microscopic mechanism gained from the MD simulations has been used as an input of the microscopic theory [81] for description of light-induced

deformations in side-chain azobenzene polymers. It is the first time when the internal architecture of azobenzene macromolecules, i.e. orientation distribution of chromophores with respect to the main chain, is explicitly taken into account. The microcopic theory satisfies all three criteria for a proper choice of the light induced force established from the analysis of select experiments:

1. The force is found to be strong enough to deform irreversibly a glassy polymer film,
2. The sign of the force is very sensitive to the molecular architecture,
3. The force decreases with temperature.

For some architectures, the theory predicts a non-monotonic dependence of sample elongation on the light intensity, the effect found experimentally [44, 48]. It stays to be checked whether this new microscopic approach correctly predicts some other interesting phenomena. For example, the present theory covers also description of molecular glasses made of isolated chromophores [86, 99]. According to the microscopic theory, a sample should be uniaxially compressed along the polarization vector, since the chromophores orient perpendicular to this vector.

MD simulations revealed a strong influence of liquid-crystalline effects on the deformation behaviour nor only in the case of LC polymer but also in the case of amorphous polymer [26–28]. Therefore, it is planned to extend the present microscopic approach to take into account the effects of LC interactions between chromophores. Another interesting development would be a study of effects of long-chain elasticity and cross-linking in azobenzene elastomers.

ACKNOWLEDGEMENTS

MS would like to express her deep gratitude to Norman Mechau from Karlsruhe Institute of Technology, to Padmanabh U. Veer and Ullrich Pietsch from Siegen University, to Burkhard Stiller and Dieter Neher from Potsdam University, to Gerhard Heinrich from Institute of Polymer Research Dresden. Without their warm attitude and everyday readiness to share the knowledge and ideas, this review will not be ever published.

The work was supported by the DFG grants NE410/8-1, NE410/8-2 and the RFBR grant 08-03-00150.

REFERENCES

[1] Sainova, D., Zen, A., Nothofer, H.-G., Asawapirom, U., Scherf, U., Hagen, R., Bieringer, T., Kostromine, S. and Neher, D. Photoaddressable alignment layers for fluorescent polymers in polarized electroluminescence devices. *Adv. Funct. Mat.* **12** (2002), 49–57.

[2] Zen, A., Neher, D., Bauer, C., Asawapirom, U., Scherf, U., Hagen, R., Kostromine, S. and Mahrt, R. F. Polarization-selective photoconductivity in aligned polyfluorene layers. *Appl. Phys. Lett*. **80** (2002), 4699–4701.

[3] Viswanathan, N. K., Kim, D. Y., Bian, S., Williams, J., Liu, W., Li, L., Samuelson, L., Kumar, J. and Tripathy, S. K. Surface relief structures on azo polymer films. *J. Mater. Chem*. **9** (1999), 1941–1955.

[4] Natansohn, A., Rochon, P. Photoinduced motions in azobenzene-based amorphous polymers: possible photonic devices. *Adv. Mater*. **11** (1999), 1387–1391.

[5] Berg, R. H., Hvilsted, S. and Ramanujam, P. S. Peptide oligomers for holographic data storage. *Nature* **383** (1996), 505–508.

[6] Rasmussen, P. H., Ramanujam, P. S., Hvilsted, S. and Berg, R. H. A remarkably efficient azobenzene peptide for holographic information storage. *J. Am. Chem. Society* **121** (1999), 4738–4743.

[7] Zilker, S. J., Bieringer, T., Haarer, D., Stein, R. S., van Egmond, J. W. and Kostromine, S. G. Holographic data storage in amorphous polymers. *Adv. Mater*. **10** (1998), 855–859.

[8] Stracke, A., Wendorff, J. H., Goldmann, D., Janietz, D. and Stiller, B. Gain effects in optical storage: thermal induction of a surface relief grating in a smectic liquid crystal. *Adv. Mater*. (2000), 282–285.

[9] Stiller, B., Geue, T., Morawetz, K. and Saphiannikova, M. Optical patterning in azobenzene polymer films. *J. Micros*. **219** (2005), 109–114.

[10] Finkelmann, H., Nishikawa, E., Pereira, G. G. and Warner, M. A new opto-mechanical effect in solids. *Phys. Rev. Lett*. **87** (2001), 015501, 1–4.

[11] Camacho-Lopez, M., Finkelmann, H., Palffy-Muhoray, P. and Shelly, M. Fast liquid-crystal elastomer swims into the dark. *Nature Mater*. **3** (2004), 307–310.

[12] Yu, Y. L., Nakano, M. and Ikeda, T. Direct bending of polymer film by light – Miniaturizing of a simple photochemical system could expand its range of applications. *Nature* **425** (2003), 145–145.

[13] Yi, D. K., Kim, M. J. and Kim, D.-Y. *Langmuir* **18** (2002), 2019–2023.

[14] Henneberg, O., Morawetz, K., Schulz, B., Dietzel, B., Saphiannikova, M., Roth, M. and Pietsch, U. 2D and 3D buried gratings made from azobenzene-polymer multilayer films. *Proc. SPIE* **6343** (2006), 634337, 1–12.

[15] Eich, M., Wendorff, J. H., Reck, B. and Ringsdorf, H. Reversible digital and holographic optical storage in polymeric liquid-crystals. *Makromol. Chem. Rapid Commun*. **8** (1987), 59–63.

[16] Eich, M., Wendorff, J. H. Erasable holograms in polymeric liquid-crystals. *Makromol. Chem. Rapid Commun*. **8** (1987), 467–471.

[17] Todorov, T., Nikolova, L. and Tomova, N. Polarization holography. 1. A new high-efficiency organic material with reversible photoinduced birefringence. *Appl. Opt*. **23** (1984), 4309–4312.

[18] Todorov, T., Nikolova, L. and Tomova, N. Polarization holography. 2. Polarization holographic gratings in photoanisotropic materials with and without intrinsic birefringence. *Appl. Opt*. **23** (1984), 4588–4591.

[19] Todorov, T., Nikolova, L., Stoyanova, K. and Tomova, N. Polarization holography. 3. Some applications of polarization holographic recording. *Appl. Opt*. **24** (1985), 785–788.

[20] Rochon, P., Batalla, E. and Natansohn, A. Optically induced surface gratings on azoaromatic polymer films. *Appl. Phys. Lett*. **66** (1995), 136–138.

[21] Kim, D. Y., Tripathy, S. K., Li, L. and Kumar, J. Laser-induced holographic surface relief gratings on nonlinear optical polymer films. *Appl. Phys. Lett*. **66** (1995), 1166–1168.

[22] Barrett, C., Rochon, P. and Natansohn, A. Mechanism of optically inscribed high-efficiency diffraction gratings in Azo polymer films. *J. Phys. Chem*. **100** (1996), 8836–8842.

[23] Kim, D. Y., Li, L., Jiang, X. L., Shivshankar, V., Kumar, J. and Tripathy, S. K. Polarized laser induced holographic surface relief gratings on polymer films. *Macromolecules* **28** (1995), 8835–8839.

[24] Bublitz, D., Helgert, M., Fleck, B., Wenke, L., Hvilstedt, S. and Ramanujam, P. S. Photoinduced deformation of azobenzene polyester films. *Appl. Phys. B* **70** (2000), 863–865.

[25] Holme, N. C. R., Nikolova, L., Hvilsted, S., Rasmussen, P. H., Berg, R. H. and Ramanujam, P. S. Optically induced surface relief phenomena in azobenzene polymers. *Appl. Phys. Lett*. **74** (1999), 519–521.

[26] Ilnytskyi, J., Saphiannikova, M. and Neher, D. Photo-induced deformations in azobenzene-containing side-chain polymers: Molecular dynamics study. *Cond. Matter Phys*. **9** (2006), 87–94.

[27] Ilnytskyi, J. M., Neher, D. Structure and internal dynamics of a side chain liquid crystalline polymer in various phases by molecular dynamics simulations: A step towards coarse graining. *J. Chem. Phys*. **126** (2007), 174905, 1–12.

[28] Ilnytskyi, J., Neher, D., Saphiannikova, M., Wilson, M. R. and Stimson, L. Molecular dynamics simulations of various branched polymeric liquid crystals. *Mol. Cryst. Liq. Cryst*. **496** (2008), 186–201.

[29] Oliveira Jr. O. N., Kumar, J., Li, L. and Tripathy, S. K. Surface-relief gratings on azobenzene-containing films. in *Photoreactive Organic Thin Films* Z. Sekkat and, W. Knoll (eds). Elsevier Science, Vol. 560, 2002.

[30] Whitten, D. G., Chen, L. H., Geiger, H. C., Perlstein, J. and Song, X. D. Self-assembly of aromatic-functionalized amphiphiles: The role and consequences of aromatic-aromatic noncovalent interactions in building supramolecular aggregates and novel assemblies. *J. Phys. Chem. B* **102** (1998), 10098–10111.

[31] Kim, B. J., Park, S. Y. and Choi, D. H. Effect of molecular aggregation on the photo-induced anisotropy in amorphous polymethacrylate bearing an aminonitroazobenzene moiety. *Bull. Korean Chem. Soc*. **22** (2001), 271–275.

[32] Hoeben, F. J. M., Jonkheijm, P., Meijer, E. W. and Schenning, A. P. H. J. About supramolecular assemblies of p-conjugated systems. *Chem. Rev*. **105** (2005), 1491–1546.

[33] Yu, Y. L., Nakano, M., Shishido, A., Shiono, T. and Ikeda, T. Effect of cross-linking density on photoinduced bending behavior of oriented liquid-crystalline network films containing azobenzene. *Chem. Mater*. **16** (2004), 1637–1643.

[34] Hvilsted, S., Ramanujam, P. S. The azobenzene optical storage puzzle – demands on the polymer scaffold? *Monatshefte für Chemie* **132** (2001), 43–51.

[35] Börger, V.: Maßgeschneiderte azobenzolhaltige Polymere für Untersuchungen zum photoinduzierten Massetransport. Braunschweig University, 2004.

[36] Freiberg, S., Lagugne-Labarthet, F., Rochon, P. and Natansohn, A. Synthesis and characterization of a series of azobenzene-containing side-chain liquid crystalline polymers. *Macromolecules* **36** (2003), 2680–2688.

[37] Mechau, N.: Lichtinduziertes Erweichen azobenzolhaltiger Polymerfilme. PhD Thesis, Potsdam University, 2005.

[38] Galvan-Gonzalez, A., Belfield, K. D., Stegeman, G. I., Canva, M., Chan, K.-P., Park, K., Sukhomlinova, L. and Twieg, R. J. Photostability enhancement of an azobenzene photonic polymer. *Appl. Phys. Lett*. **77** (2000), 2083–2085.

[39] Srikhirin, T., Cimrova, V., Schiewe, B., Tzolov, M., Hagen, R., Kostromine, S., Bieringer, T. and Neher, D.. An investigation of the photoinduced changes of absorption of high-performance photoaddressable polymers. *Chem. Phys. Chem*. **3** (2002), 335–342.

[40] Geue, T., Schultz, M., Grenzer, J., Pietsch, U., Natansohn, A. and Rochon, P. X-ray investigations of the molecular mobility within polymer surface gratings. *J. Appl. Phys*. **87** (2000), 7712–7719.

[41] Pietsch, U., Rochon, P. and Natansohn, A. Formation of a buried lateral density grating in azobenzene polymer films. *Adv. Mater*. **12** (2000), 1129–1132.

[42] Barrett, C. J., Rochon, P. L. and Natansohn, A. L. Model of laser-driven mass transport in thin films of dye-functionalized polymers. *J. Chem. Phys*. **109** (1998), 1505–1516.

[43] Borger, V., Menzel, H. and Huber, M. R. Influence of the molecular weight of azopolymers on the photo-induced formation of surface relief gratings. *Mol. Cryst. Liq. Cryst*. **430** (2005), 89–97.

[44] Fukuda, T., Matsuda, H., Shiraga, T., Kimura, T., Kato, M., Viswanathan, N. K., Kumar J. and Tripathy, S. K. Photofabrication of surface relief grating on film of azobenzene polymers with different dye functionalization. *Macromolecules* **33** (2000), 4220–4225.

[45] Andruzzi, L., Altomare, A., Ciardelli, F., Solaro, R., Hvilsted, S. and Ramanujam, P. S. Holographic gratings in azobenzene side-chain polymethacrylates. *Macromolecules* **32** (1999), 448–454.

[46] Yager, K. G., Barrett, C. J. Temperature modeling of laser-irradiated azo-polymer thin films. *J. Chem. Phys*. **120** (2004), 1089–1096.

[47] Kumar, J., Li, L., Jiang, X. L., Kim, D.-Y., Lee, T. S. and Tripathy S. Gradient force: The mechanism for surface releif grating formation on azobenzene functionalized polymers. *Appl. Phys. Lett*. **72** (1998), 2096–2098.

[48] Bian, S., Williams, J. M., Kim, D. Y., Li, L., Balasubramanian, S., Kumar, J. and Tripathy, S. Photoinduced surface deformations on azobenzene polymer films. *J. Appl. Phys*. **86** (1999), 4498–4508.

[49] Baldus, O., Leopold, A., Hagen, R., Bieringer, T. and Zilker, S. J. Surface relief gratings generated by pulsed holography: A simple way to polymer nanostructures without isomerizing side-chains. *J. Chem. Phys*. **114** (2001), 1344–1349.

[50] Baldus, O., Zilker, S. J. Surface relief gratings in photoaddressable polymers generated by cw holography. *Appl. Phys. B* **72** (2001), 425–427.

[51] Saphiannikova, M., Geue, T. M., Henneberg, O., Morawetz, K. and Pietsch, U. Linear viscoelastic analysis of formation and relaxation of azobenzene polymer gratings. *J. Chem. Phys*. **120** (2004), 4039–4045.

[52] Lefin, P., Fiorini, C. and Nunzi, J.-M. Anisotropy of the photo-induced translational diffusion of azobenzene dyes in polymer matrices. *Pure Appl. Opt*. **7** (1998), 71–82.

[53] Lefin, P., Fiorini, C. and Nunzi, J. M. Anisotropy of the photoinduced translation diffusion of azo-dyes. *Opt. Mater*. **9** (1998), 323–328.

[54] Bellini, B., Ackermann, J., Klein, H., Grave, C., Dumas, P. and Safarov V. Light-induced molecular motion of azobenzne-containing molecules: a random-walk model. *J. Phys.: Condens. Matter* **18** (2006), 1817–1835.

[55] Geue, T., Ziegler, A. and Stumpe, J. Light-induced orientation phenomena in Langmuir-Blodgett multilayers. *Macromolecules* **30** (1997), 5729–5738.

[56] Jung, C. C., Rosenhauer, R., Rutloh, M., Kempe, C. and Stumpe, J. The generation of three-dimensional anisotropies in thin polymer films by angular selective photoproduct formation and annealing, *Macromolecules* **38** (2005), 4324–4330.

[57] Kulinna, C., Hvilsted, S., Hendann, C., Siesler, H. W. and Ramanujam, P. S. Selectively deuterated liquid crystalline cyanoazobenzene side-chain polyesters. 3. Investigations of laser induced segmental mobility by Fourier transform infrared spectroscopy. *Macromolecules* **31** (1998), 2141–2151.

[58] Yaroschuk, O., Sergan, T., Lindau, J., Lee, S. N., Kelly, J. and Chien, L. C. Light induced structures in liquid crystalline side-chain polymers with azobenzene functional groups. *J. Chem. Phys*. **114** (2001), 5330–5337.

[59] Sekkat, Z., Dumont, M. Photoinduced orientation of azo dyes in polymeric films – characterization of molecular angular mobility. *Synth. Met*. **54** (1993), 373–381.

[60] Dumont, M., Osman, A. E. On spontaneous and photoinduced orientational mobility of dye molecules in polymers. *Chem. Phys*. **245** (1999), 437–462.

[61] Pedersen, T. G., Johansen, P. M., Holme, N. C. R., Ramanujam, P. S. and Hvilsted, S. Mean-Field Theory of Photoinduced Formation of Surface Relief in Side-Chain Azobenzene Polymers. *Phys. Rev. Lett*. **80** (1998), 89–92.

[62] Bublitz, D., Fleck, B. and Wenke, L. A model for surface-relief formation in azobenzene polymers. *Appl. Phys. B* **72** (2001), 931–936.

[63] Gaididei, Y. B., Christiansen, P. L. and Ramanujam, P. S. Theory of photoinduced deformation of molecular films. *Appl. Phys. B* **74** (2002), 139–146.

[64] Lee, J. D., Kim, M. J. and Nakayama, T. A single-dipole model of surface relief grating formation on azobenzene polymer films. *Langmiur* **24** (2008), 4260–4264.

[65] Srikhirin, T., Laschitsch, A., Neher, D. and Johannsmann, D. Light-induced softening of azobenzene dye-doped polymer films probed with quartz crystal resonators. *Appl. Phys. Lett*. **77** (2000), 963–965.

[66] Mechau, N., Neher, D., Börger, V., Menzel, H. and Urajama, K. Optically driven diffusion and mechanical softening in azobenzene polymer layers. *Appl. Phys. Lett*. **81** (2002), 4715–4717.

[67] Mechau, N., Saphiannikova, M. and Neher, D. Dielectric and mechanical properties of azobenzene polymer layers under visible and ultraviolet irradiation. *Macromolecules* **38** (2005), 3894–3902.

[68] Grenzer, M. Photoinduced material transport in amorphous azobenzene polymer films. Habil. thesis, Potsdam University, 2007.

[69] Mechau, N., Saphiannikova, M. and Neher, D. Molecular tracer diffusion in thin azobenzene polymer layers. *Appl. Phys. Lett*. **89** (2006), 251902.

[70] Bublitz, D., Fleck, B., Wenke, L., Ramanujam, P. S. and Hvilsted, S. Determination of the response time of photoanisotropy in azobenzene side-chain polyesters. *Optics Communication* **182** (2000), pp. 155–160.

[71] Veer, P. U., Pietsch, U., Rochon, P. L. and Saphiannikova, M. Temperature dependent analysis of grating formation on azobenzene polymer films. *Mol. Cryst. Liq. Cryst*. **486** (2008), 1108–1120.

[72] Veer, P. U., Pietsch, U. and Saphiannikova, M. Time and temperature dependence of surface relief grating formation in polymers containing azobenzene groups with different dipole moments. *J. Appl. Phys*. **106** (2009), 014909, 1–7.

[73] Strobl, G. R. *The Physics of Polymers*. Springer, Berlin, 1997.

[74] Cicerone, M. T., Blackburn, F. R. and Ediger, M. D. Anomalous diffusion of probe molecules in polystyrene – evidence for spatially heterogeneous segmental dynamics. *Macromolecules* **28** (1995), 8224–8232.

[75] Tseng, K. C., Turro, N. J. and During, C. J. Tracer diffusion in thin polystyrene films. *Polymer* **41** (2000), 4751–4755.

[76] van Keuren, E., Schrof, W. Fluorescence Recovery after Two-Photon Bleaching for Study of Dye Diffusion in Polymer Systems. *Macromolecules* **36** (2003), 5002–5007.

[77] Sperling, L. H. *Introduction to Physical Polymer Science*. John Wiley & Sons, Inc., New York, 1992.

[78] Gimenez, R., Millaruelo, M., Pinol, M., Serrano, J. L., Vinuales, A., Rosenhauer, R., Fischer, T. and Stumpe, J. Synthesis, thermal and optical properties of liquid crystalline terpolymers containing azobenzene and dye moieties. *Polymer* **46** (2005), 9230–9242.

[79] Karageorgiev, P., Neher, D., Schulz, B., Stiller, B., Pietsch, U., Giersig, M. and Brehmer, L. From anisotropic photo-fluidity towards nanomanipulation in the optical near-field. *Nature Mater*. **4** (2005), 699–703.

[80] Saphiannikova, M., Neher, D. Thermodynamic theory of light-induced material transport in amorphous azobenzene polymer films. *J. Phys. Chem. B* **109** (2005), 19428–19436.

[81] Toshchevikov, V. P., Saphiannikova, M. and Heinrich, G. Microscopic theory of light-induced deformation in amorphous side-chain azobenzene polymers. *J. Phys. Chem. B* **113** (2009), 5032–5045.

[82] Geue, T. M., Saphiannikova, M. G., Henneberg, O., Pietsch, U., Rochon, P. L. and Natansohn, A. L. Formation mechanism and dynamics in polymer surface gratings. *Phys. Rev. E* **65** (2002), 052801,1–4.

[83] Gay, J. G., Berne, B. J. Modification of the overlap potential to mimic a linear site-site potential. *J. Chem. Phys*. **74** (1981), 3316–3319.

[84] Yamamoto, T., Hasegawa, M., Kanazawa, A., Shiono, T. and Ikeda, T. Phase-type gratings formed by photochemical phase transition of polymer azobenzene liquid crystals: Enhancement of diffraction efficiency by spatial mdulation of mlecular aignment. *J. Phys. Chem. B* **103** (1999), 9873–9878.

[85] Collings, P. J., Hird, M. *Introduction to Liquid Crystals*. Taylor & Francis, London, 2001.

[86] Fuhrmann, T., Tsutsui, T. Synthesis and properties of a hole-conducting, photopatternable molecular glass. *Chem. Mater*. **11** (1999), 2226–2232.

[87] Yager, K. G., Barrett, C. J. Photomechanical surface patterning in azo-polymer materials. *Macromolecules* **39** (2006), 9320–9326.

[88] Lifshitz, E. M., Landau, L. D. *Electrodynamics of Continuous Media*. Nauka, Moscow, 1982.

[89] Wang, X. J. Theoretical descriptions of nematic polymers, networks and gels. *Prog. Polym. Sci*. **22** (1997), 735–764.

[90] Gotlib, Y. Y., Torchinskii, I. A. and Toshchevikov, V. P Effects of nematic ordering on the relaxation spectrum of a polymer network with included rod-like particles: Mean-field approximation. *Macromol. Theory Simul*. **13** (2004), 303–317.

[91] Toshchevikov, V. P., Gotlib, Y. Y. Shear dynamic modulus of nematic elastomers: Modified Rouse model. *Macromolecules*. **42** (2009), 3417–3429.

[92] Chigrinov, V., Pikin, S., Verevochnikov, A., Kozenkov, V., Khazimullin, M., Ho, J., Huang, D. D. and Kwok, H. S. Diffusion model of photoaligning in azo-dye layers. *Phys. Rev. E* **69** (2004), 061713.

[93] Shibaev, V., Bobrovsky, A. and Boiko, N. Photoactive liquid crystalline polymer systems with light-controllable structure and optical properties. *Prog. Polym. Sci*. **28** (2003), 729–836.

[94] Landau, L. D., Lifshitz, E. M. *Theory of Elasticity*. Elsevier Science Ltd, 1981.

[95] Heermann, D. W. *Computer Simulation Methods in Theoretical Physics*. Springer, Berlin, 1990.

[96] Rubinstein, M., Colby, R. H. *Polymer Physics*. Oxford University Press, Oxford, 2003.

[97] Ilnytskyi, J., Wilson, M. R. A domain decomposition molecular dynamics program for the simulation of flexible molecules with an arbitrary topology of Lennard-Jones and/or Gay-Berne sites. *Comput. Phys. Commun*. **134** (2001), 23–32.

[98] Ilnytskyi, J., Wilson, M. R. A domain decomposition molecular dynamics program for the simulation of flexible molecules of spherically-symmetrical and nonspherical sites. II. Extension to NVT and NVP ensembles. *Comput. Phys. Commun*. **148** (2002), 43–58.

[99] Shirota, Y. Photo- and electroactive amorphous molecular materials - molecular design, syntheses, reactions, properties, and applications. *J. Mater. Chem*. **15** (2005), 75–93.